Journal of Comparative Physiology B (2019) 189:549–566
https://doi.org/10.1007/s00360-019-01231-x

ORIGINAL PAPER

An in vitro analysis of intestinal ammonia transport in fasted and fed freshwater rainbow trout: roles of NKCC, K^+ channels, and Na^+, K^+ ATPase

Julian G. Rubino[1] · Jonathan M. Wilson[2] · Chris M. Wood[1,3]

Received: 19 March 2019 / Revised: 15 July 2019 / Accepted: 21 August 2019 / Published online: 5 September 2019

Abstract

We examined mechanisms of ammonia handling in the anterior, mid, and posterior intestine of unfed and fed freshwater rainbow trout (*Oncorhynchus mykiss*), with a focus on the Na^+:K^+:2Cl^- co-transporter (NKCC), Na^+:K^+-ATPase (NKA), and K^+ channels. NKCC was localized by immunohistochemistry to the mucosal (apical) surface of enterocytes, and NKCC mRNA was upregulated after feeding in the anterior and posterior segments. NH_4^+ was equally potent to K^+ in supporting NKA activity in all intestinal sections. In vitro gut sac preparations were employed to examine mucosal ammonia flux rates (Jm_{amm}, disappearance from the mucosal saline), serosal ammonia flux rates (Js_{amm}, appearance in the serosal saline), and total tissue ammonia production rates ($Jt_{amm} = Js_{amm} - Jm_{amm}$). Bumetanide ($10^{-4}$ mol L^{-1}), a blocker of NKCC, inhibited Js_{amm} in most preparations, but this was largely due to reduction of Jt_{amm}; Jm_{amm} was significantly inhibited only in the anterior intestine of fed animals. Ouabain (10^{-4} mol L^{-1}), a blocker of NKA, generally reduced both Jm_{amm} and Js_{amm} without effects on Jt_{amm} in most preparations, though the anterior intestine was resistant after feeding. Barium (10^{-2} mol L^{-1}), a blocker of K^+ channels, inhibited Jm_{amm} in most preparations, and Js_{amm} in some, without effects on Jt_{amm}. These pharmacological results, together with responses to manipulations of serosal and mucosal Na^+ and K^+ concentrations, suggest that NKCC is not as important in ammonia absorption as previously believed. NH_4^+ appears to be taken up through barium-sensitive K^+ channels on the mucosal surface. Mucosal NH_4^+ uptake via both NKCC and K^+ channels is energized by basolateral NKA, which plays an additional role in scavenging NH_4^+ on the serosal surface to possibly minimize blood toxicity or enhance ion uptake and amino acid synthesis following feeding. Together with recent findings from other studies, we have provided an updated model to describe the current understanding of intestinal ammonia transport in teleost fish.

Keywords Feeding · Intestine · Sodium · Potassium · Gut sac

Introduction

Ammoniotelic fish, such as rainbow trout (*Oncorhynchus mykiss*), excrete ammonia as their primary nitrogenous waste product, mainly through the gills (Wilkie 2002; Ip and Chew 2010). The gills, followed by the kidney, have received the primary focus in terms of mechanistic analyses for ammonia handling, whereas the gut has received relatively little attention. This is surprising considering that ammonia excretion increases greatly after feeding (e.g., Brett and Zala 1975; Bucking and Wood 2008; Zimmer et al. 2010), and intestinal digestive processes create an abundant ammonia source. Notably, chyme (the partially digested food matter within the intestine) has been shown to contain approximately 1–2 mmol l^{-1} ammonia (or higher) following a meal in various teleost species (Bucking and Wood 2012; Bucking et al. 2013a; Rubino et al. 2014; Pelster et al. 2015; Wood et al. 2019), which represents a significant ammonia challenge to the system, considering that this concentration is an order of magnitude greater than normal plasma levels (Bucking and Wood 2008, 2012). Indeed, after feeding in

Communicated by B. Pelster.

✉ Julian G. Rubino
rubinojg@gmail.com

[1] McMaster University, 1280 Main St. West, Hamilton, ON L8S4K1, Canada

[2] Wilfrid Laurier University, 75 University Avenue West, Waterloo, ON N2L3C5, Canada

[3] University of British Columbia, 6270 University Blvd., Vancouver, BC V6T1Z4, Canada

rainbow trout, plasma ammonia levels increase greatly in the hepatic portal vein which connects the intestinal drainage to the liver (Karlsson et al. 2006), suggesting that ammonia is absorbed from the chyme and/or synthesized within the intestinal tissue. Using an in vitro gut sac technique, Rubino et al. (2014) demonstrated that both processes occur, and their measurements suggested that close to half of the whole animal ammonia excretion after feeding could originate from the combination of these two processes. Similar observations were made using the plainfin midshipman (*Porichthys notatus*), a marine teleost (Bucking et al. 2013a).

Although it is becoming clearer that ammonia is absorbed across the intestine in teleosts, the possible mechanisms remain poorly understood. Rhesus (Rh) glycoproteins (ammonia channels) are expressed in mammalian intestine (Handlogten et al. 2005; Weiner 2006; Worrell et al. 2008). At least one Rh glycoprotein occurs in the trout intestine (Rhbg, a basolateral ammonia channel), and its mRNA expression increases in response to both feeding and high ammonia exposure (Nawata et al. 2007; Bucking and Wood 2012). In addition, Bucking et al. (2013b) demonstrated immunohistochemical localization of multiple Rh isoforms along the intestine of the plainfin midshipman. Rubino et al. (2015) observed mucosa to serosa transport of an Rh-permeable analogue, ^{14}C-methylammonia, in competition with ammonia in trout gut sacs, further suggesting Rh glycoprotein involvement. In a preliminary pharmacological survey, Rubino et al. (2015) also reported that the Na^+:K^+:$2Cl^-$ (NKCC) co-transporter inhibitor bumetanide (applied mucosally), as well as the Na^+:K^+ ATPase (NKA) inhibitor ouabain (applied serosally) and low [Na^+] treatments (applied to both surfaces simultaneously) inhibited the serosal flux of ammonia (Js_{amm}, i.e., appearance in the serosal solution). A variety of other Na^+ transport blockers (applied mucosally for Na^+:H^+ exchange, Na^+ channels, and H^+-ATPase) were without effect on Js_{amm}. These results suggested the involvement of active transport, overall Na^+ dependence, and the specific involvement of NKCC, which would contribute to the Na^+ dependence. However, Rubino et al. (2015) studied only preparations from fed fish and did not measure either the mucosal flux of ammonia (Jm_{amm}, i.e., disappearance from the mucosal solution) or the endogenous ammonia production rate ($Jt_{amm} = Js_{amm} - Jm_{amm}$) of the intestinal tissue, so alternate interpretations are possible. These might include undetected responses in Jm_{amm} and/or Jt_{amm}, and/or mechanisms that are only present when induced by feeding.

In the present study, we again used the in vitro trout gut sac system to investigate in greater detail the Na^+ dependence, as well as possible K^+ dependence, of intestinal ammonia transport, with parallel experiments on fed and fasted animals. The focus on K^+ originated from the bumetanide results of Rubino et al. (2015) in which ammonia flux (but only Js_{amm} was measured) was reduced by this inhibitor, as well as the known ability of NH_4^+ to substitute for K^+ in other systems. For example, in mammalian models, NH_4^+ can directly substitute for K^+ on NKCC, which is postulated as a dominant mechanism of ammonia uptake (Worrell et al. 2008). The ammonium ion (NH_4^+) shares a similar hydrated ionic radius and charge as K^+, and, therefore, may compete with K^+ for binding to a variety of transport proteins, including NKCC, NKA, and K^+ channels (reviewed by Abdoun et al. 2007; Ip and Chew 2010). Specific experiments focused on the effects of altered [Na^+] and [K^+] concentrations, ouabain, bumetanide, and the general K^+-channel blocker barium on simultaneous measurements of Jm_{amm}, Jt_{amm}, and Js_{amm}. We also examined the mRNA expression and immunohistochemical localization of NKCC in fasted and fed fish, as well as the ability of NH_4^+ to support intestinal NKA activity, in replacement of K^+.

Our specific hypotheses were that trans-intestinal ammonia fluxes would be perturbed by both [Na^+] and [K^+] manipulations, as well as by treatments with ouabain, barium, and bumetanide, and that responses would differ between preparations from fed and unfed trout. In particular, we hypothesized that evidence supporting a key role for NKCC in ammonia transport would be obtained, such as inhibition of Jm_{amm} by bumetanide, by low mucosal [Na^+], and stimulation by high mucosal [Na^+] and low mucosal [K^+]. We also predicted that that NKCC would be localized to the apical (mucosal) surface by immunohistochemistry in this freshwater species, which would complement findings from marine teleost fish (summarized by Grosell 2011), and that its mRNA expression would increase with feeding. We also predicted that NH_4^+ would be able to successfully replace K^+ in activation of intestinal NKA activity. Overall, the present study advances our understanding of ammonia transport in the teleost intestine.

Materials and methods

Experimental animals

Rainbow trout (*Oncorhynchus mykiss*, 150–250 g from Humber Springs Trout Hatchery, Ontario, Canada, were kept in 500-L tanks (density of 30 fish per tank), with a flow-through (1.8 L min^{-1}) of dechlorinated Hamilton tapwater (moderately hard). Composition (in mequiv L^{-1}) was [Na^+] = 0.6, [Cl^-] = 0.8, [Ca^{2+}] = 1.8, [Mg^{2+}] = 0.3, [K^+] = 0.05; titration alkalinity = 2.1; pH ~ 8.0; hardness ~ 140 mg L^{-1} as $CaCO_3$ equivalents; temperature = 12.5–14 °C, background ammonia concentration ≤ 10 µmol L^{-1}). Fish were on a maintenance feeding regime, administered as approximately 3% of their body mass fish three times per week (Martin Profishent Aquaculture Nutrition, Tavistock, ON, Canada; crude

protein 45%, crude fat 9%, crude fiber 3.5%) and allowed to acclimate for 4 weeks prior to experiments. All procedures followed the regulations outlined by the Canada Council for Animal Care under McMaster University Animal Utilization Protocol 09-04-10.

In vitro gut sac experiments

Gut sac experiments were performed to quantify ammonia fluxes using mucosal and serosal solutions of varying composition, with methods similar to those of Rubino et al. (2014). A common protocol was employed across all treatments. In unfed treatments, trout were fasted for 1 week prior to experimentation. Fed trout were of same group as the unfed fish; however, they were given a single satiating meal (~3–5% body mass) and allowed 24 h to digest. In each group, randomly selected fish were euthanized with a terminal overdose of 0.07 g L^{-1} pH-neutralized MS222. The body cavity was revealed through a ventral midline incision from the pectoral fins to the anus. The entire gut was then excised, freed from connective and adipose tissue, and placed in an ice-cold bath of Cortland saline (Wolf 1963; in mmol L^{-1}: NaCl 124, KCl 5.1, $CaCl_2$ 1.6, $MgSO_4$ 0.9, $NaHCO_3$ 11.9, NaH_2PO_4 3, glucose 5.5, pH = 7.4). The bile duct was tied off using 2-0 silk to prevent bile spillover into the intestine. The entire gut was flushed internally with Cortland saline to remove chyme. The whole intestine from a single fish was used for a given treatment and the anterior, mid, and posterior intestines were separated from each other, and tied off at one end. A flared polyethylene tube (Intramedic Clay-Adams PE-60; Becton-Dickenson and Company, Sparks, MD) was inserted into the open end and tied in place with 2-0 silk. The desired mucosal saline, depending upon the treatment (see below), was then infused into each individual gut section via syringe. Repeated withdrawal and reinfusion ensured thorough mixing. A small volume of this mixed solution was taken, marked as the initial mucosal solution, and stored at − 20 °C for later analysis. Sections were filled with saline until taut, at a similar tension to that of a fed intestine filled with chyme, and the tube was sealed. The control mucosal solution was Cortland saline modified to contain 1 mmol L^{-1} ammonium chloride (NH_4Cl), which was previously determined to be a physiologically relevant concentration of ammonia in chyme 24-h post-feeding (Rubino et al. 2014). The sacs were rinsed with Cortland saline, blotted dry, weighed to 0.0001 g accuracy for initial weight (W_i), and then immersed into 15-mL (mid and posterior intestines) or 50-mL (anterior intestine) plastic centrifuge tubes containing saline, which varied in composition depending upon the treatment (see below). This saline was termed the serosal solution. Control serosal saline was an unmodified Cortland saline.

A 2-h flux period began upon submersion of the sacs into their respective serosal solutions. Serosal solutions were bubbled with a 99.7% O_2:0.3% CO_2 gas mixture for the entire flux period, mimicking physiological PCO_2 (2.25 Torr) as well as maximizing O_2 availability. At the end of the 2-h flux, gut sacs were immediately removed, and a 5-ml sample of the serosal solution stored at − 20 °C for future analysis. Sacs were then blotted dry and weighed again (W_f), and the mucosal solution was collected and stored at − 20 °C for future analysis. The empty preparation was thoroughly blotted again and weighed again for empty weight (W_e). Surface area of the tissue was then measured, using graph paper as outlined by Grosell and Jensen (1999), and as done in our previous studies (Rubino et al. 2014, 2015) and many others (e.g., Nadella et al. 2014; Pelster et al. 2015). These surface area measurements did not incorporate contributions of luminal villi or intestinal folds. Control treatments were conducted in parallel with all the series listed below.

Series 1: Na^+ series

Treatments of ouabain, low mucosal and serosal [Na^+] (LSMN), and high mucosal [Na^+] (HMN) were employed.

For the ouabain treatment, 10^{-4} mol L^{-1} ouabain was added to both the serosal and mucosal solutions. Ouabain was dissolved in a small volume of Cortland saline through heating, and then added to the stock solution used in the experiments. The concentration of ouabain used in this study is within the range used in other in vitro studies (e.g., rat astrocyte cultures, Hosoi et al. 2002; trout gill NKA activity assays McCormick 1993).

In the LSMN series, NaCl was removed from the Cortland saline in both the mucosal and serosal solutions and substituted with the inert osmolyte mannitol. This reduced [Na^+] to about 15 mmol L^{-1}. The osmolality was carefully balanced by adding mannitol until the exact target value was achieved, as measured using an osmometer (Wescor 5100C; Logan, UT, USA), so that it was the same in mucosal and serosal solutions, and like that of an unmodified Cortland saline. NaCl was reduced on both sides, because earlier studies demonstrated rapid backflux of Na^+ from the serosal to mucosal solutions if the serosal concentration was not reduced simultaneously (e.g. Nadella et al. 2014).

HMN treatment involved doubling the NaCl concentration to 248 mmol L^{-1}, yielding a [Na^+] of about 263 mequiv L^{-1} in the mucosal solution. Osmolality of the serosal solution was again balanced using mannitol and confirmed using an osmometer, so that it was the same as in the mucosal solution. This was done to ensure that any differences were observed because of increased [Na^+] only, and not through differences in osmotic pressure.

Series 2: bumetanide

Bumetanide (10^{-4} mol L^{-1}) was added only to the mucosal solution. The concentration of bumetanide used in this study is similar to that used previously in fish epithelial transport studies (e.g. Marshall 1986). The drug was first dissolved in a carrier solvent, DMSO, and then added to Cortland saline, so that the final mucosal solution contained 0.1% DMSO. The serosal solution was Cortland saline modified to contain only 0.1% DMSO. Control treatments in this series used Cortland saline modified to contain 0.1% DMSO in both the mucosal and serosal solutions to assess for any differences in fluxes emerging solely from the use of DMSO. Differences in osmolality were negligible.

Series 3: K^+ series

Low mucosal [K^+] (LMK), low serosal [K^+] (LSK), high mucosal barium (HMB), and high serosal barium (HSB) treatments were employed. In the LMK and LSK treatments, KCl was not added to the mucosal or serosal saline, respectively, which is represented by the treatment names. Osmolality was balanced using a small amount of mannitol. In the high barium treatments, 10^{-2} mol L^{-1} $BaCl_2$ was added to either the mucosal or serosal saline, and osmolality was again balanced using mannitol. It is known that this high level of Ba^{2+} is needed to block many K + channels when applied externally (Yellen 1987; Taglialatela et al. 1993).

Analytical procedures

Ammonia

Collected mucosal samples were thawed, and immediately deproteinized using ice-cold 20% perchloric acid. Samples were then pH neutralized using 1 mol L^{-1} KOH. Quantification of ammonia in the serosal and deproteinized mucosal solutions were performed using a commercial assay (Raichem Cliniqa ammonia assay, glutamate dehydrogenase method) modified for use in a microplate (read at 340 nm) by scaling down the reagents used in the assay. Standard curves were generated for every group of measured samples. Samples and standards were treated similarly.

NKA activity

After trout were fasted for a week, they were fed a single satiating meal, and euthanized 24 h later via terminal overdose of neutralized MS-222. This same protocol was used for the fed treatments for NKCC mRNA expression and immunohistochemistry (see below). Samples of the gill, anterior, mid, and posterior intestine were taken, rinsed with Cortland saline as above, flash frozen in liquid N_2, and stored at − 80 °C for the NKA assay. Frozen tissue was homogenized in an ice-cold EGTA-deoxycholate buffer and NKA activity was determined based on a protocol established by McCormick (1993). Activity was normalized to protein content determined via a commercial assay (Bio-Rad, Hercules, CA, USA), using a standard curve based on bovine serum albumin (Sigma, St. Louis, MO, USA).

NKCC mRNA expression

Total RNA was extracted from homogenized anterior, mid, and posterior intestine samples of unfed and fed fish using TriZol (Invitrogen, Burlington, ON). Total RNA was quantified, and purity was measured spectrophotometrically (Nanodrop ND-1000, Nanodrop Technologies, Wilmington, DE, USA). RNA integrity was then assessed by running samples on a 1% agarose gel stained with RedSafe (FroggaBio, Toronto, ON). The cDNA was synthesized using an oligo(dT17) primer, and Superscript II reverse transcriptase (Invitrogen, Burlington, ON). The mRNA expression levels of NKCC1a (GenBank: DQ864492) were then determined from this synthesized cDNA using quantitative polymerase chain reaction (qPCR) using the following primer pair:

Forward: 5′-AAC TTT GTG GAT CCG AGT GG-3′
Reverse: 5′-TAT CAG CTT GTC CCC CAG AG-3′.

Reactions were 20 µl consisting of 4 µL of 5 × diluted cDNA, 4 pmol of both forward and reverse primers, 0.8 µl of 10× diluted ROX dye, and 10 µL of SYBR Green (Bio-Rad) and were performed using an MX3000P qPCR System (Stratagene, Cedar Creek, TX). To verify the formation of a single PCR product, melt curve analysis was performed on the samples, alongside no template controls, and non-reverse transcribed controls. Relative gene expression was generated from a standard curve, through serial dilution of a randomly selected sample, and was normalized to β-actin, which was expressed equally in unfed and fed fish.

Immunohistochemistry

Anterior and posterior intestine segments were excised from unfed and fed fish. Cross-sectional rings (< 0.5 cm) were cut and immersion-fixed in 10% neutral buffered formalin solution, pH 7.3 overnight at 4 °C and then stored in 70% ethanol. Tissue was later processed for paraffin embedding, and sectioned (5 µm). Sections were collected on APS (aminopropylsilane) coated slides and immunolabelled as described in Wilson et al. (2007).

Briefly, sections were dewaxed, and antigen retrieval performed (0.05% citraconic anhydride pH 7.3 for 30 min at 100 °C) and blocked with 5% normal goat serum in 0.05% Tween-20/phosphate-buffered saline, pH 7.4 (TPBS).

Sections were probed with the NKCC/NCC mouse monoclonal antibody T4 (1:100; Xu et al. 1994; Hiroi et al. 2005) alone or in combination with the pan-specific NKA-α subunit rabbit polyclonal antibody αR1 (1:500; Wilson et al. 2007) overnight at 4 °C. Following a series of rinsing steps with TPBS, sections were incubated with goat anti-mouse Dylight 594 and goat anti-rabbit Alexa Fluor 488 (1:500, both from Jackson ImmunoResearch Laboratories, West Grove, PA, USA) for 1 h at 37 °C. Following rinsing with TPBS, nuclei were counter-stained with DAPI (4′,6-diamidino-2-phenylindole) and coverslips mounted with 1:1 glycerol:PBS. Sections were viewed and images were collected with a Leica DM6000B photomicroscope (Wetzlar, Germany).

Calculations

Serosal and mucosal ammonia flux rates

To calculate the serosal ammonia flux rate (Js_{amm}, in μmol cm^{-2} h^{-1}, i.e., appearance in the serosal saline), the following formula was used:

$$Js_{amm} = \left[\left(Ts_{ammf} - Ts_{ammi}\right)\right] \times Vs]/SA \times t, \quad (1)$$

where Ts_{ammf} and Ts_{ammi} are the final, and initial ammonia concentrations (μmol L^{-1}) in the serosal solution, Vs is the volume of the serosal solution (L), SA is the surface area of the intestinal sac (cm^2), and t is time (h). All fluxes were positive, indicating flux of ammonia into the serosal saline.

The mucosal ammonia flux rate (Jm_{amm}, in μmol cm^{-2} h^{-1}, i.e., disappearance from the mucosal saline) was calculated using the following formula:

$$Jm_{amm} = \left[\left(Tm_{ammi} \times Vm_i\right) - \left(Tm_{ammf} \times Vm_f\right)\right]/SA \times t, \quad (2)$$

where Tm_{ammf} and Tm_{ammi} are the final and initial ammonia concentrations (μmol L^{-1}) in the mucosal solution, and Vm_f and Vm_i are the final and initial volumes of the mucosal solution (L). Vm_f was calculated as $W_f - W_e$, and Vm_i as $W_i - W_e$ (In vitro gut sac experiments, above). Positive Jm_{amm} fluxes indicate ammonia flux out of the mucosal solution, whereas negative fluxes represent ammonia flux into the mucosal solution.

Total tissue ammonia production rates

Total tissue ammonia production rates (Jt_{amm}; μmol cm^{-2} h^{-1}), representing the net rate of endogenous ammonia production by the gut tissue, was calculated using the formula:

$$Jt_{amm} = Js_{amm} - Jm_{amm}. \quad (3)$$

The calculation assumes that there is no net change in tissue ammonia content. Rubino et al. (2014) suggested that this assumption is valid, as tissue ammonia content remained unchanged over the duration of their gut sac experiments.

Statistical analyses

Data have been expressed as mean ± SEM (N number of fish). In Table 1, comparisons made between control unfed and control fed fish (significant differences represented by asterisks), and between controls, and DMSO controls (significant differences represented by daggers) were conducted using a Student's unpaired t test with Bonferroni correction. Controls across all treatments were pooled for these analyses. In Figs. 1, 2, 3, 4, 5, 6, 7, 8, and 9, comparisons made between controls (of either unfed or fed fish) and experimental treatments within Series 1, 2, or 3 (significant differences represented by asterisks) were conducted by a one-way ANOVA, followed

Table 1 Control and DMSO control Js_{amm}, Jm_{amm}, and Jt_{amm} values for the anterior, mid, and posterior intestine of unfed and fed fish

	Unfed control	Fed control	Unfed DMSO	Fed DMSO
Js_{amm}				
Anterior	0.23 ± 0.01 (N = 10)	0.21 ± 0.02 (N = 10)	0.15 ± 0.004† (N = 6)	0.21 ± 0.01* (N = 6)
Mid	0.15 ± 0.01 (N = 12)	0.18 ± 0.01* (N = 9)	0.08 ± 0.01† (N = 6)	0.12 ± 0.01†, * (N = 6)
Posterior	0.23 ± 0.02 (N = 5)	0.16 ± 0.01 (N = 5)	0.05 ± 0.01† (N = 6)	0.09 ± 0.01* (N = 6)
Jm_{amm}				
Anterior	0.07 ± 0.03 (N = 8)	0.09 ± 0.03 (N = 6)	0.004 ± 0.01 (N = 6)	0.019 ± 0.003* (N = 4)
Mid	0.07 ± 0.03 (N = 7)	0.08 ± 0.01 (N = 7)	− 0.01 ± 0.003 (N = 5)	0.003 ± 0.01† (N = 4)
Posterior	0.09 ± 0.02 (N = 5)	0.09 ± 0.02 (N = 5)	− 0.0007 ± 0.03† (N = 4)	0.01 ± 0.01† (N = 6)
Jt_{amm}				
Anterior	0.16 ± 0.03 (N = 8)	0.12 ± 0.04 (N = 6)	0.15 ± 0.01 (N = 6)	0.19 ± 0.01†,* (N = 4)
Mid	0.08 ± 0.03 (N = 7)	0.10 ± 0.01 (N = 7)	0.09 ± 0.01 (N = 5)	0.12 ± 0.01 (N = 4)
Posterior	0.14 ± 0.03 (N = 5)	0.07 ± 0.02* (N = 5)	0.05 ± 0.03† (N = 4)	0.08 ± 0.01 (N = 6)

Values are mean ± SE. Flux values were measured in μmol/cm^2/h

*Significant difference ($P < 0.05$) between unfed and fed fish

†Significant difference ($P < 0.05$) between controls and DMSO controls

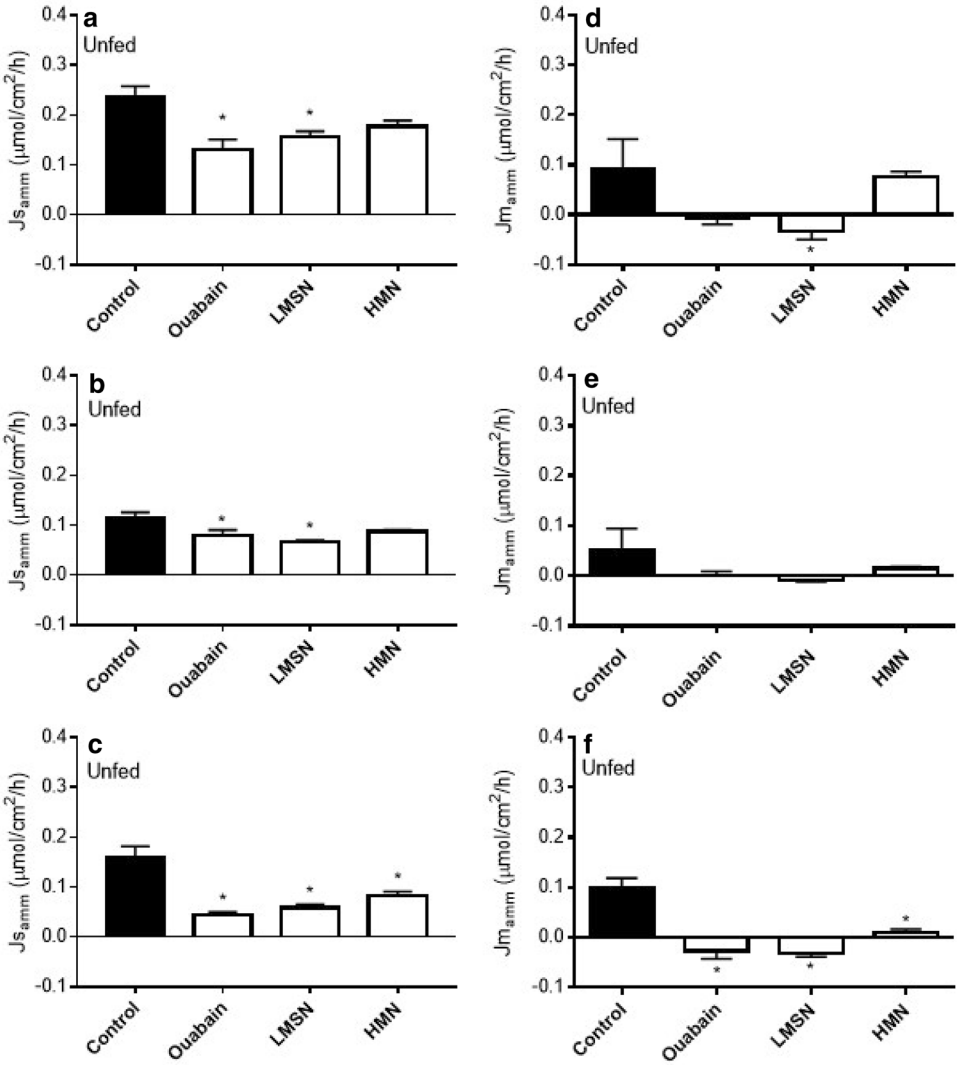

Fig. 1 Serosal (Js_{amm}) and mucosal (Jm_{amm}) ammonia flux rates (μmol/cm^2/h) of the anterior (**a** $N=5, 4, 5, 4$, **d** $N=4, 4, 4, 4$), mid (**b** $N=6, 5, 5, 5$, **e** $N=4, 4, 4, 4$), and posterior intestine (**c** $N=5, 5, 5, 5$, **f** $N=5, 4, 4, 4$) of unfed fish for the Na^+ series. Exposures included unfed controls (black bars) and unfed ouabain, low mucosal and serosal sodium (LMSN), and high mucosal sodium (HMN) treatments (white bars). "Asterisk" significant ($P<0.05$) comparing the unfed treatments to the unfed controls

by Dunnett's post hoc test. In Table 2, for the NKA activity analysis, comparisons in activities made between K^+ and NH_4^+ at the same concentration (significant differences represented by asterisks) were conducted via Student's unpaired *t* test, while comparisons of NKA activity among different intestinal sections (significant differences represented by letters) were conducted by a repeated-measures ANOVA. For the NKCC gene expression, comparisons made between unfed and fed fish (significant differences indicated by asterisks) were conducted by a Student's unpaired *t* test. In all cases, significance was accepted at the $P<0.05$ level.

Results

The effect of feeding and DMSO on Js_{amm}, Jm_{amm}, and Jt_{amm}

Under control conditions, feeding elicited a significant increase in Js_{amm} only in the mid intestine (Table 1). Similarly, Jm_{amm} remained unchanged in all sections in response to feeding; however, Jt_{amm} was significantly decreased in the fed posterior intestine. When 0.1% DMSO

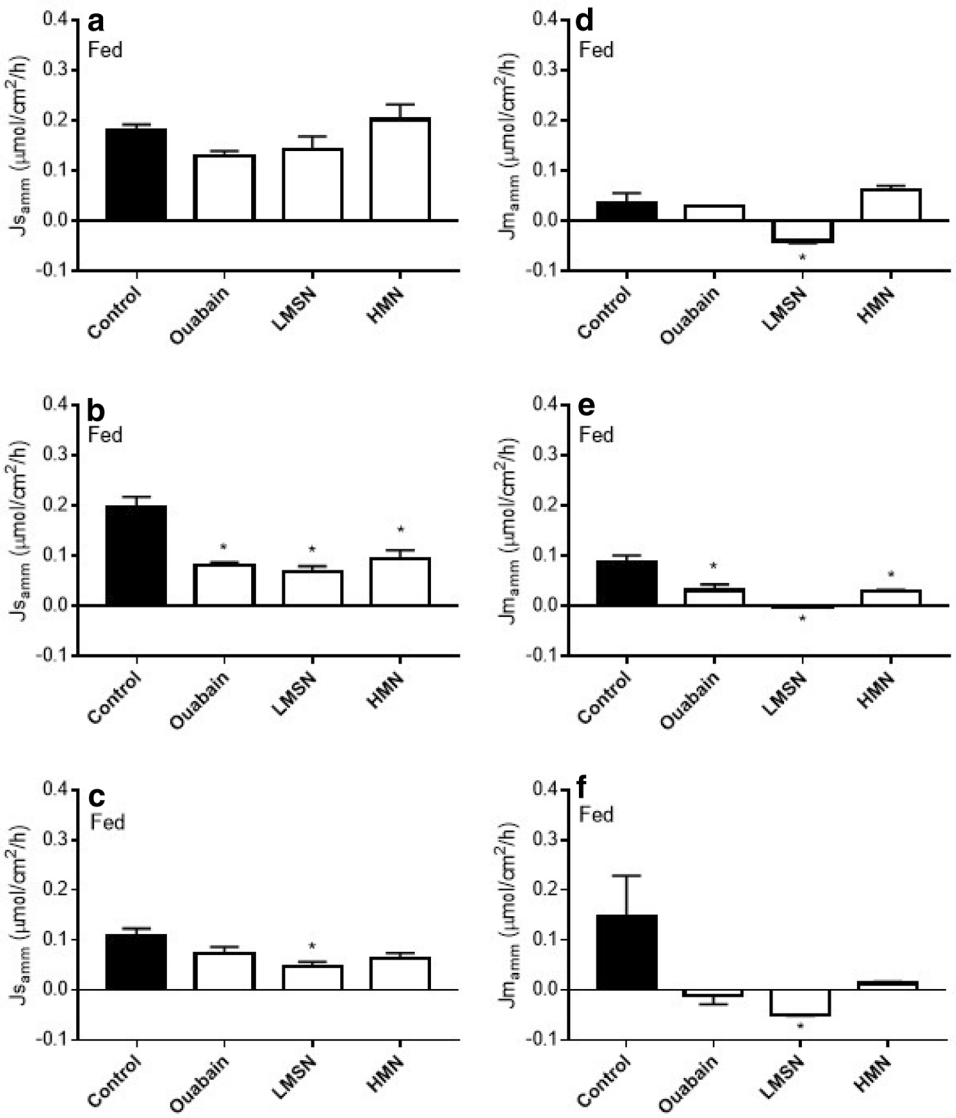

Fig. 2 Serosal (Js_{amm}) and mucosal (Jm_{amm}) ammonia flux rates (μmol/cm^2/h) of the anterior (**a** $N=5, 4, 4, 4$, **d** $N=3, 4, 4, 4$), mid (**b** $N=4, 5, 4, 4$, **e** $N=3, 4, 4, 4$), and posterior intestine (**c** $N=5, 5, 4, 4$, **f** $N=5, 3, 4, 4$) of fed fish for the Na^+ series. Exposures included fed controls (black bars) and fed ouabain, low mucosal and serosal sodium (LMSN), and high mucosal sodium (HMN) treatments (white bars). "Asterisk" Significant ($P<0.05$) comparing the fed treatments to the fed controls

was present, Js_{amm} was significantly reduced in all sections in unfed fish, with a similar trend for Jm_{amm}, but the latter was significant only in the posterior intestine. The inhibitory effect of DMSO on ammonia transport was still present in fed fish (significant for Js_{amm} in mid intestine, and for Jm_{amm} in mid and posterior intestine). Feeding significantly increased Js_{amm} in all three sections in the presence of DMSO, with a similar trend in Jm_{amm}, but the latter was significant only in the anterior intestine. Notably, in the presence of DMSO, only Jt_{amm} of the anterior intestine was significantly increased in fed fish.

Na^+ series

Ouabain (10^{-4} mol L^{-1}) significantly decreased Js_{amm} in all sections in unfed fish (Fig. 1), with decreases ranging from 75% in the posterior intestine (Fig. 1c), to 27% in the mid intestine (Fig. 1b). Ouabain also essentially eliminated or even reversed Jm_{amm} in all sections, though the effect was significant only in the posterior intestine (Fig. 1f). This inhibitory effect of ouabain on ammonia transport was less pronounced in fed fish, where significant decreases in both Js_{amm} and Jm_{amm} were observed only in the mid intestine (Fig. 2b, e). Jt_{amm} was not significantly affected by ouabain in any section, under either unfed or fed conditions (Fig. 3).

The effects of the LMSN treatment were generally very similar to those of ouabain. LMSN caused significant decreases in Js_{amm} of all intestinal sections in unfed fish (Fig. 1a–c). These decreases, compared to controls, ranged from 33% in the anterior intestine (Fig. 1a), to 63% in the posterior intestine (Fig. 1c). LMSN similarly eliminated or even reversed Jm_{amm} in all sections of unfed fish, though the inhibition was significant only in the anterior and posterior intestines (Fig. 1d, f). Fed fish also

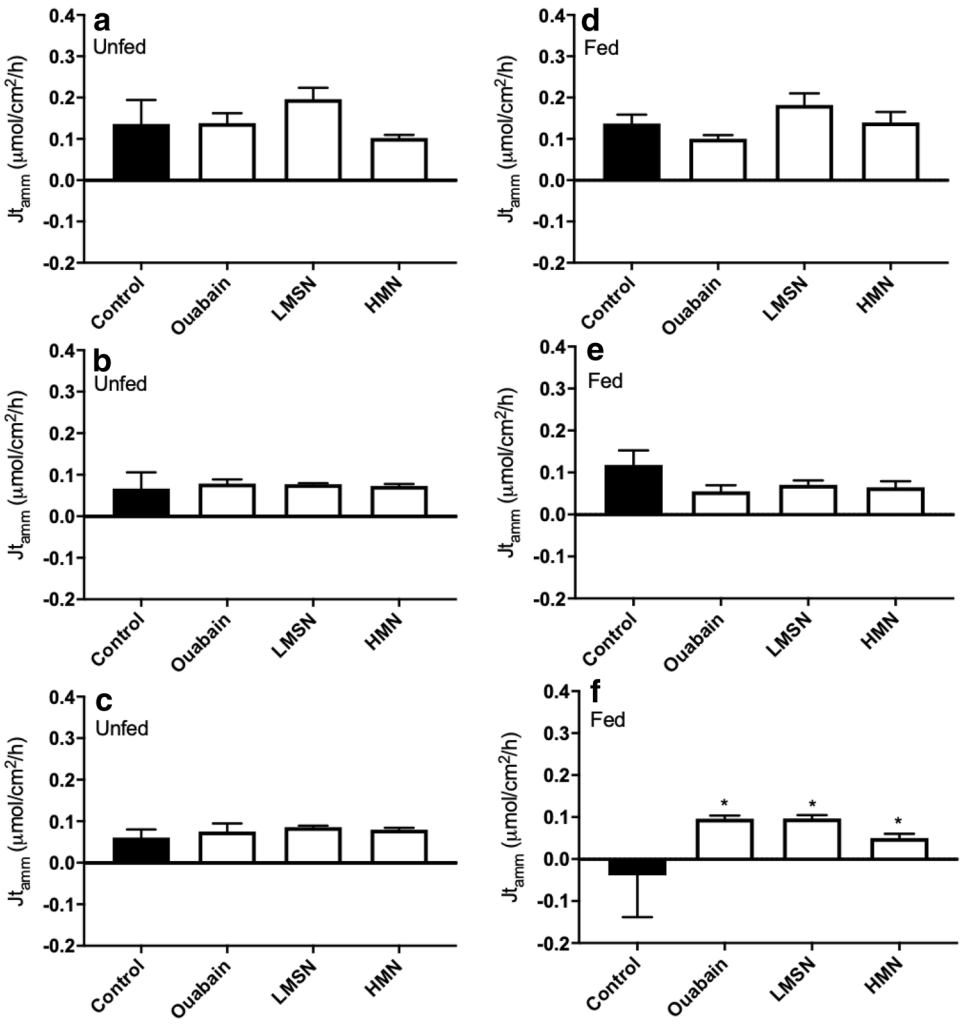

Fig. 3 Total tissue ammonia production rates (Jt_{amm}: μmol/cm^2/h) of the anterior (**a** $N=4$, 4, 4, 4, **d** $N=3$, 4, 4, 4), mid (**b** $N=4$, 4, 4, 4, **e** $N=3$, 4, 4, 4), and posterior intestine (**c** $N=5$, 4, 4, 4, **f** $N=5$, 3, 4, 4) of unfed and fed fish for the Na^+ series. Exposures included unfed and fed controls (black bars) and unfed and fed ouabain, low mucosal and serosal sodium (LMSN), and high mucosal sodium (HMN) treatments (white bars). "Asterisk" significant ($P<0.05$) comparing the unfed and fed treatments to the respective unfed and fed controls

experienced decreases in Js_{amm}, with significant effects in the mid and posterior intestine (Fig. 2b, c). LMSN exposure had more profound inhibitory effects on Jm_{amm} compared to those of ouabain in fed fish, with elimination or reversal of flux in all three sections (Fig. 2d–f). As with ouabain, Jt_{amm} was not significantly affected by LMSN in any section, under either unfed or fed conditions (Fig. 3).

HMN was generally inhibitory to ammonia transport, but did not have as large of an impact as observed with ouabain and LMSN treatments. In unfed fish, significant decreases in both Js_{amm} and Jm_{amm} were observed only in the posterior intestine (Fig. 1c, f). In fed fish, the mid intestine was the only section to experience decreases in both Js_{amm} and Jm_{amm} with HMN treatment (Fig. 2b, e). HMN had no significant effect on Jt_{amm} in any section, under either fed or unfed conditions, similar to the preceding two treatments (Fig. 3).

Bumetanide series

DMSO (0.1%) was required as a vehicle for bumetanide (10^{-4} mol L^{-1}). As DMSO in itself caused significant effects on ammonia transport (see above, Table 1), all bumetanide responses were evaluated relative to the DMSO control treatment. Bumetanide had strong inhibitory effects on Js_{amm} in all three sections in unfed fish (Fig. 4a–c), without significant effects on Jm_{amm} except in the anterior intestine where Jm_{amm} was actually elevated (Fig. 4d). These actions of bumetanide correlated with marked reductions in Jt_{amm} in all sections which were significant only in the anterior and mid intestine (Fig. 6a, b). In general, qualitatively similar effects of bumetanide (reductions in Js_{amm} and Jt_{amm}, unchanged Jm_{amm}) were seen in fed fish (Figs. 5, 6), though feeding abolished the significant reductions in Js_{amm} (Fig. 4a) and Jt_{amm} (Fig. 6a) seen in the anterior intestine of unfed fish and

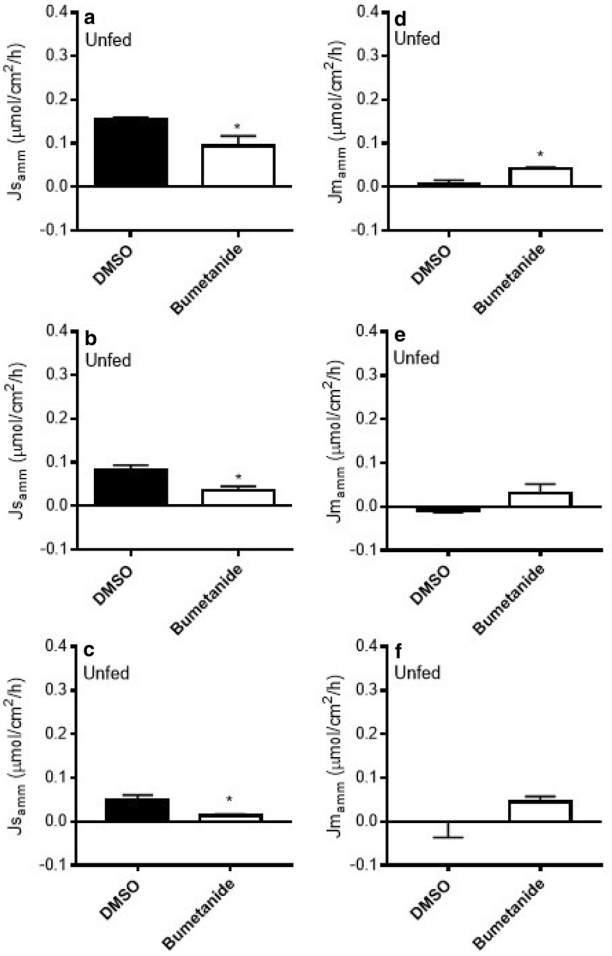

Fig. 4 Serosal (Js_{amm}) and mucosal (Jm_{amm}) ammonia flux rates (µmol/cm^2/h) of the anterior (**a** $N=5$, 4, **d** $N=5$, 4), mid (**b** $N=5$, 5, **e** $N=5$, 4), and posterior (**c** $N=5$, 5, **f** $N=4$, 4) intestine of unfed fish for the DMSO and bumetanide treatments. Exposures included unfed DMSO controls (black bars) and unfed bumetanide treatment (white bars). "Asterisk" significant ($P<0.05$) comparing the unfed bumetanide treatment to the unfed DMSO control treatment

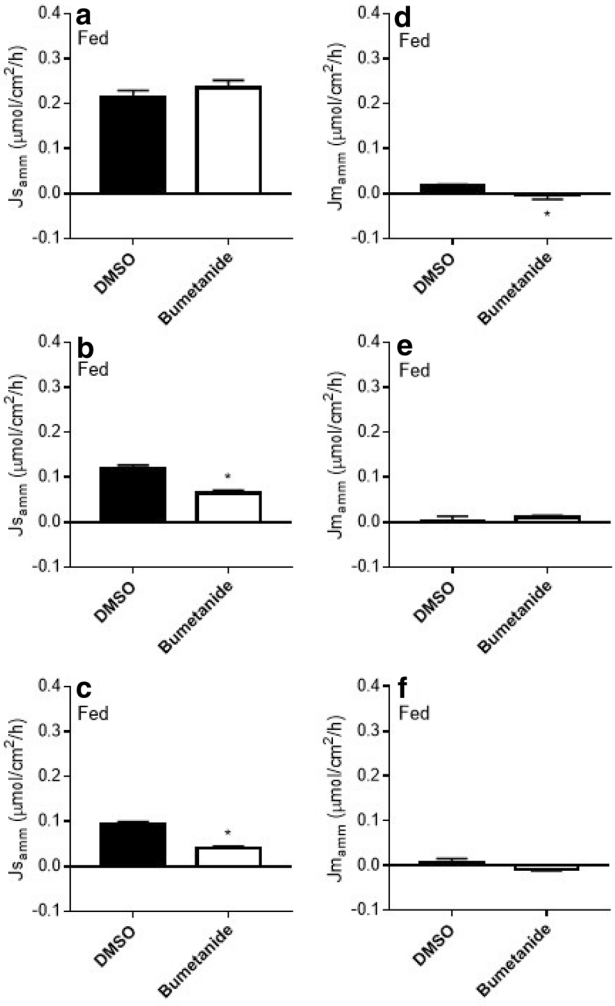

Fig. 5 Serosal (Js_{amm}) and mucosal (Jm_{amm}) ammonia flux rates (µmol/cm^2/h) of the anterior (**a** $N=5$, 5, **d** $N=4$, 4), mid (**b** $N=5$, 5, **e** $N=4$, 4), and posterior (**c** $N=5$, 5, **f** $N=5$, 4) intestine of fed fish for the DMSO and bumetanide treatments. Exposures included fed DMSO controls (black bars) and fed bumetanide treatment (white bars). "Asterisk" significant ($P<0.05$) comparing the fed bumetanide treatment to the fed DMSO control treatment

reversed the stimulation of Jm_{amm} (Fig. 4d) to a slight but significant inhibition (Fig. 5d).

K^+ series

Compared to the Na^+ series (cf. Figs. 1, 2), the treatments employed in this series had less profound impacts on Js_{amm} throughout the intestine, whereas virtually all of them markedly inhibited Jm_{amm}, except in the anterior segment of unfed fish (Figs. 7, 8).

In unfed fish, LMK significantly inhibited Js_{amm} only in the posterior intestine, with a 61% decrease from the control value (Fig. 7c). However, LMK essentially eliminated Jm_{amm} in the mid and posterior intestine (Fig. 7e, f) but was without effect in the anterior intestine (Fig. 7d). In fed fish, LMK had no significant effects on Js_{amm} in any section (Fig. 8a–c), whereas Jm_{amm} was again inhibited, with virtual total blockade in the anterior and posterior segments (Fig. 8d, f). LMK had no significant effects on Jt_{amm} in any section (Fig. 9).

LSK showed generally similar responses LMK. In unfed fish, there was a comparable significant decrease in Js_{amm} only in the posterior intestine (Fig. 7c), and a virtual elimination of Jm_{amm} only in the mid and posterior intestine (Fig. 7e, f). In fed fish, Js_{amm} was again unaffected by LSK in all sections (Fig. 8a–c), whereas Jm_{amm} was reduced or reversed in all sections (Fig. 8d–f). Again, Jt_{amm} was generally unaltered throughout, except for an increase in the fed posterior intestine (Fig. 9).

Responses to HMB and HSB treatments were virtually identical. In unfed as well as fed trout, there was

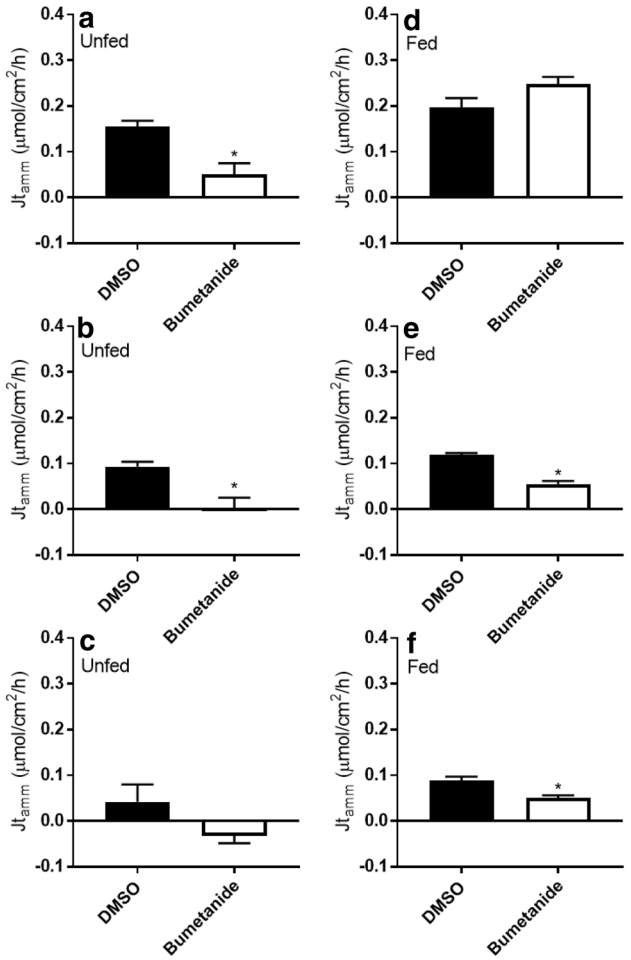

Fig. 6 Total tissue ammonia production rates (Jt_{amm}: μmol/cm^2/h) of the anterior (**a** $N=5$, 4, **d** $N=4$, 4), mid (**b** $N=5$, 4, **e** $N=4$, 4), and posterior intestine (**c** $N=4$, 4, **f** $N=4$, 4) of unfed and fed fish for the DMSO and bumetanide treatments. Exposures included unfed and fed DMSO controls (black bars) and unfed and fed bumetanide treatment (white bars). "Asterisk" significant ($P<0.05$) comparing the unfed and fed bumetanide treatments to the respective unfed and fed DMSO controls

strong inhibition of Js_{amm} in the posterior intestine by both (Figs. 7c,8c), and in the mid intestine of unfed animals by HMB only (Fig. 7b). Jm_{amm} was eliminated by both HMB and HSB in the mid and posterior sections of unfed animals (Fig. 7e, f), and strongly inhibited in all three sections of fed animals (Fig. 8d–f). HMB and HSB had no effects on Jt_{amm} in any section (Fig. 9).

The effects of NH_4^+ on the activation of Na^+:K^+-ATPase

NKA activity across the whole intestine was more than an order of magnitude higher than that observed in the gills (Table 2). The ability of NH_4^+ to support NKA activity was evaluated by replacing K^+ with NH_4^+. For gill NKA, activity with both 1 mmol L^{-1} and 3 mmol L^{-1} NH_4^+ was greatly reduced relative to assays run with 1 mmol L^{-1} and 3 mmol L^{-1} K^+. However, for intestinal NKA from all three sections, activity with NH_4^+ was comparable to that with K^+ at both concentrations (Table 2).

The effects of feeding on the mRNA expression and immunohistochemical analysis of NKCC

Relative normalized gene expression for NKCC was altered by feeding status (Fig. 9). In both the anterior and posterior intestine, there were significant increases in gene expression (eightfold and fourfold, respectively) in response to feeding. Expression in the mid intestine remained unchanged.

Further exploration of the anterior and posterior intestines was performed by NKCC/NCC immunohistochemical staining (Fig. 10). The protein was apically located on the mucosal surface and feeding caused an increase in apical immunoreactivity in both sections. A stronger presence was observed in the anterior intestine compared to that of the posterior intestine. Interestingly, there was almost no appreciable apical staining in the posterior intestine of unfed fish, in contrast to the anterior intestine of unfed fish. Furthermore, no detectable immunoreaction was observed along the basal layer.

Discussion

Overview

To our knowledge, this study, together with the preliminary findings of Rubino et al. (2015), presents the first observations demonstrating a potential linkage between intestinal ion transport and ammonia handling in a fed teleost fish. As reported by Rubino et al. (2014), ammonia transport tended to increase after feeding, though in the present study, this was prominent only in the preparations where DMSO was used as a vehicle. Furthermore, feeding versus fasting resulted in rather minor differences in the responses of ammonia transport to various experimental treatments, contrary to our original hypotheses. The most prominent of these was an attenuation of the inhibitory effects of ouabain. However, manipulations of both [Na^+] and [K^+] interfered with ammonia transport, in accord with our original hypotheses, as well as the observations of Rubino et al. (2015), confirming the Na^+ dependence of ammonia transport. Furthermore, as we had predicted, increased expression of NKCC with feeding was confirmed at the mRNA level, with supporting immunohistochemical evidence. However, our specific hypothesis that NH_4^+ substitution for K^+ on apical NKCC was a key step in the mucosal uptake of ammonia was not well supported. Most importantly, mucosally applied

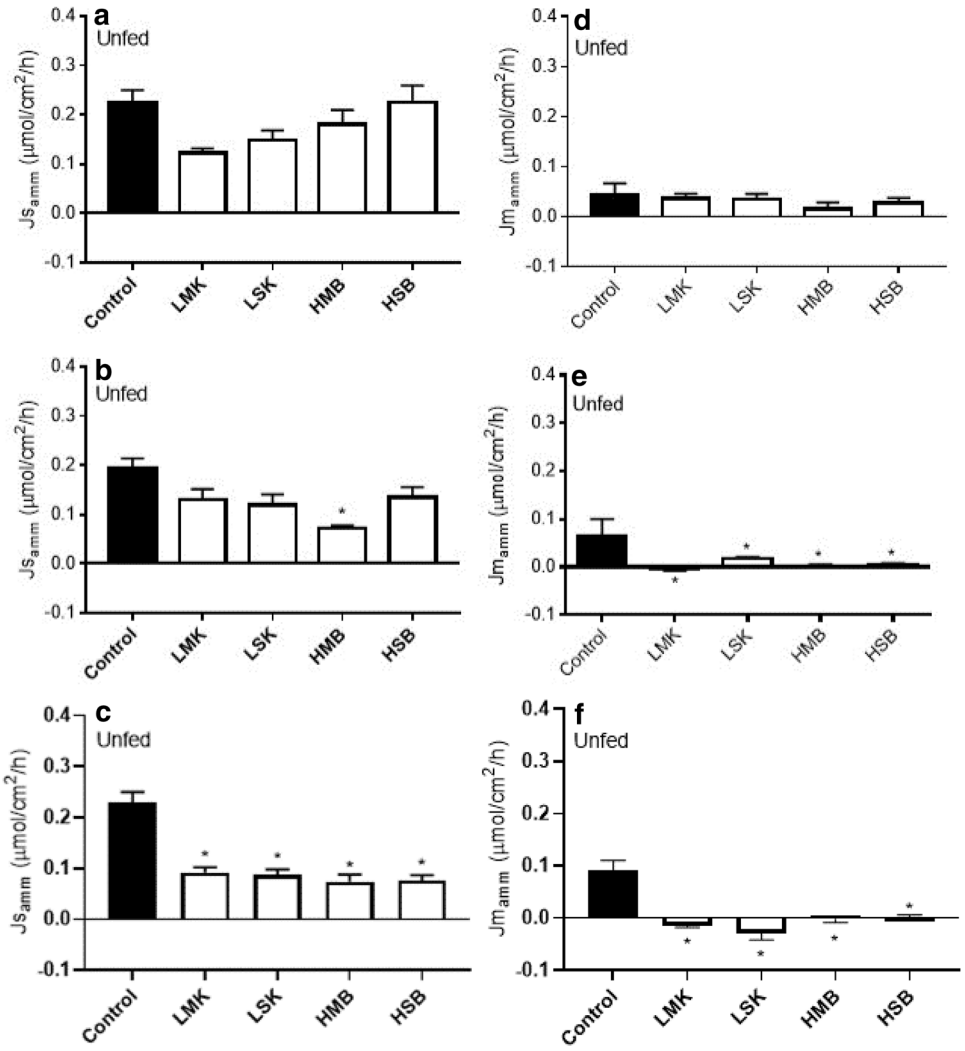

Fig. 7 Serosal (Js_{amm}) and mucosal (Jm_{amm}) ammonia flux rates (μmol/cm^2/h) of the anterior (**a** $N=4, 4, 4, 5, 5$, **d** $N=4, 5, 5, 5, 5$), mid (**b** $N=5, 5, 5, 4, 5$, **e** $N=3, 5, 5, 5, 5$), and posterior intestine (**c** $N=5, 5, 5, 5, 5$, **f** $N=5, 5, 5, 5, 5$) of unfed fish for the K^+ series. Exposures included unfed controls (black bars) and unfed low mucosal potassium (LMK), low serosal potassium (LSK), high mucosal barium (HMB), and high serosal barium (HSB) treatments (white bars). "Asterisk" significant ($P<0.05$) comparing the unfed treatments to the unfed controls

bumetanide had no detectable inhibitory effect on Jm_{amm} except in the anterior intestine of fed trout and the responses to elevated mucosal [Na^+] (HMN) and low mucosal [K^+] (LMK) were opposite to those expected if mucosal NKCC was involved. Together, the addition of Jm_{amm} and Jt_{amm} measurements to the present study, that were unavailable in Rubino et al. (2015), allowed for these observations which resulted in a change to our model. Specifically, these results highlighted less dependence on NKCC for intestinal ammonia uptake (Fig. 12). Nevertheless, an interaction with K^+ was observed. The inhibitory actions of barium indicated that this interaction probably reflected NH_4^+ passage through K^+ channels. The inhibitory effects of ouabain confirmed an important contribution of NKA to the overall transport process, and at least in part this could explain why treatments that reduced serosal [K^+] (LSK) and mucosal [Na^+] (LMSN) were also inhibitory. Finally, our hypothesis that NH_4^+ would be able to successfully replace K^+ on intestinal NKA was confirmed. This suggests that NKA also plays a role in scavenging NH_4^+ from the intestinal circulation for metabolism in the enterocytes, thereby preventing excessive increases in plasma ammonia levels after feeding. High mucosal [Na^+] (HMN) and low serosal [K^+] (LSK) would be expected to increase this basolateral "back-transport" of NH_4^+ by NKA, thereby contributing at least in part to the inhibitory effects on ammonia transport observed with these treatments.

Is NKCC involved in ammonia transport in the intestine?

NKCC mRNA was expressed in all three intestinal sections (Fig. 10) and may now be added to the list of gut transporters that are upregulated after feeding in freshwater fish (Kamunde and Wood 2003; Bucking and Wood 2012; Turner and Bucking 2017). Nadella et al. (2014) presented pharmacological evidence (inhibition of Na^+ transport by furosemide) for NKCC function in gut sacs of recently fed freshwater trout, but only in the anterior intestine; there was no effect in the mid and posterior intestine. Conversely, pharmacological

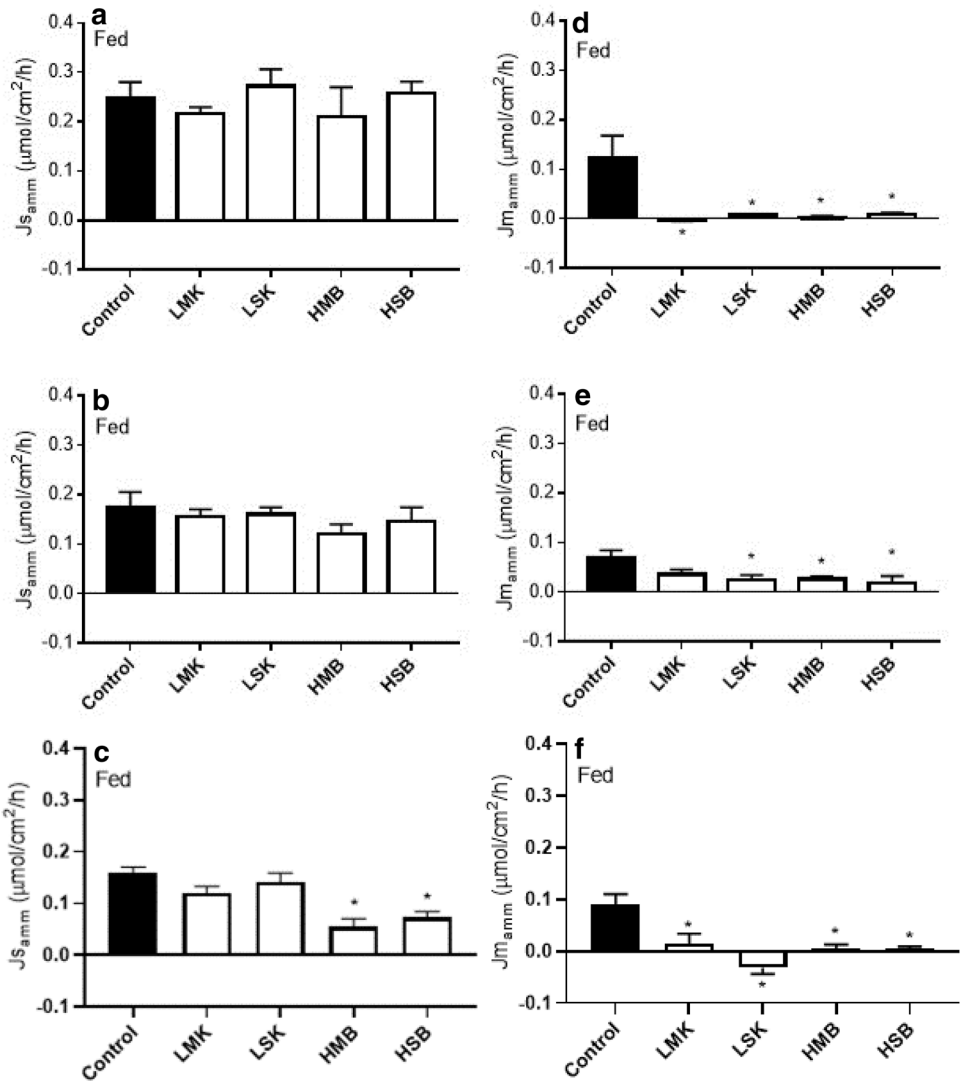

Fig. 8 Serosal (Js_{amm}) and mucosal(Jm_{amm}) ammonia flux rates (μmol/cm^2/h) of the anterior (**a** $N=4, 5, 5, 5, 5$, **d** $N=3, 4, 4, 5, 5$), mid (**b** $N=4, 4, 5, 5, 5$, **e** $N=4, 5, 5, 5, 5$), and posterior intestine (**c** $N=5, 5, 5, 5, 5$, **f** $N=5, 5, 5, 5, 5$) of fed fish for the K^+ Series. Exposures included fed controls (black bars) and fed low mucosal potassium (LMK), low serosal potassium (LSK), high mucosal barium (HMB), and high serosal barium (HSB) treatments (white bars). "Asterisk" significant ($P<0.05$) comparing the fed treatments to the fed controls

evidence (inhibition of Na^+ transport by hydrochlorothiazide) for Na^+:Cl^- co-transporter (NCC) function was seen only in the mid and posterior sacs (Nadella et al. 2014). We are aware of no other previous information on this topic in freshwater teleosts (indeed NKCC is often omitted in freshwater models—e.g. Movileanu et al. 1998), but the results fit with many studies on the gut of seawater teleosts where both NKCC and NCC are significant contributors to apical Na^+ uptake processes (reviewed by Grosell 2011). To observe if this mRNA expression resulted in detectable levels of NKCC protein expression, immunohistochemistry was performed and indicated the presence and apical location of a signal, particularly in the anterior intestine of freshwater trout. Furthermore, this signal showed increased expression after feeding, similar to the observations of increased mRNA expression following feeding (Fig. 11). One limitation in the performance of the immunohistochemistry is that the monoclonal antibody T4 which was utilized recognizes both NKCC and NCC (Xu et al. 1994). However, if, indeed, this protein is NKCC, then its apical location suggests that it would be of the absorptive type rather than the secretory type, as discussed by Hiroi et al. (2005), and in agreement with the literature on seawater teleosts (Loretz 1995; Grosell 2011). In the future, quantitatively assessing NKCC protein expression, such as through a western blot, could aid in determining the extent of the increase following feeding.

Bumetanide has been demonstrated to reduce ammonia uptake through inhibition of NKCC in multiple organ systems and cell types, including rabbit kidney (Kinne et al. 1986), mouse hybridoma cells (Westlund and Haggstrom 1998), and mouse neurons (Thrane et al. 2013). Our earlier suggestion that NKCC played a key role in intestinal ammonia transport (Rubino et al. 2015) was based on the inhibitory actions of bumetanide and low Na^+ treatments on Js_{amm}. The more detailed measurements of the present study confirmed an inhibition of Js_{amm} by both bumetanide (Figs. 4, 5) and LMSN (Figs. 1, 2) in most sections, and also showed that LMSN reduced Jm_{amm} to a comparable

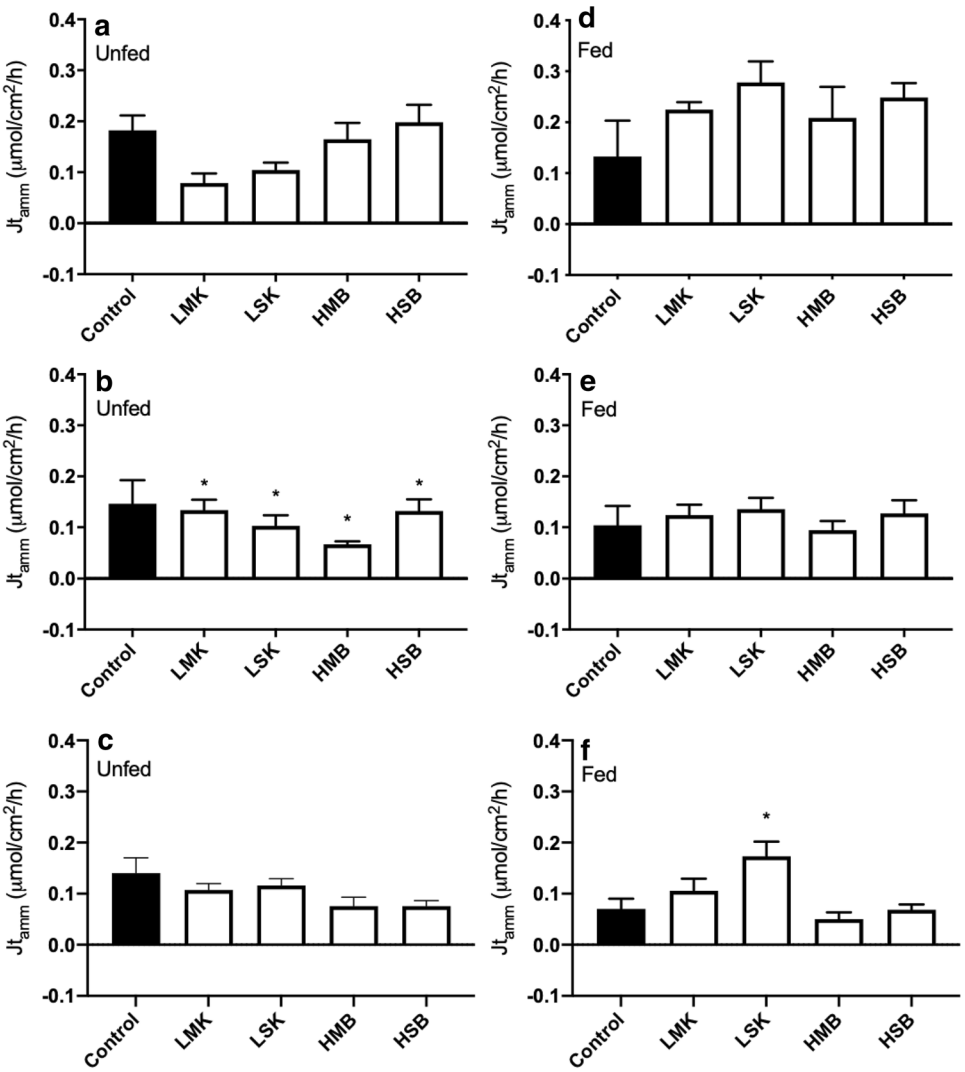

Fig. 9 Total tissue ammonia production rates (Jt_{amm}: μmol/cm^2/h) of the anterior (**a** $N=4$, 4, 4, 5, 5, **d** $N=3$, 4, 4, 5, 5), mid (**b** $N=3$, 5, 5, 4, 5, E: $N=4$, 4, 5, 5, 5), and posterior intestine (**c** $N=5$, 5, 5, 5, 5, **f** $N=5$, 5, 5, 5, 5) of unfed and fed fish for the K^+ Series. Exposures included unfed and fed controls (black bars) and unfed and fed low mucosal potassium (LMK), low serosal potassium (LSK), high mucosal barium (HMB), and high serosal barium (HSB) treatments (white bars). "Asterisk" significant ($P<0.05$) comparing the unfed and fed treatments to the respective unfed and fed controls

Table 2 Enzyme activity values for NKA in the gill, and the anterior, mid, and posterior intestine of fed fish

	1 mmol l^{-1} K^+	3 mmol l^{-1} K^+	1 mmol l^{-1} NH_4^+	3 mmol l^{-1} NH_4^+
Gill	0.21 ± 0.07	0.20 ± 0.07	0.08 ± 0.04	0.05 ± 0.01*
Anterior intestine	1.7 ± 0.4[a]	1.6 ± 0.5[a]	2.6 ± 0.8[a]	3.3 ± 1.0[a]
Mid intestine	4.1 ± 0.5[b]	1.2 ± 0.4[a]	3.1 ± 0.2[a]	2.7 ± 0.5[a]
Posterior intestine	3.7 ± 0.4[b]	2.1 ± 0.9[a]	2.8 ± 0.4[a]	3.9 ± 0.5[a]

Values are mean ± SE ($N=4$). Enzyme activity values are expressed as μmol ADP mg^{-1} protein·h^{-1}. *Significant difference ($P<0.05$) in activity levels between K^+ and NH_4^+ at the same concentration. Significant difference ($P<0.05$) among the different intestinal sections is marked with different letters

extent (Figs. 1, 2), but revealed that the inhibitory action of bumetanide on Js_{amm} can largely be explained by an inhibition of endogenous ammonia production (Jt_{amm}) by the intestinal tissue itself (Fig. 6). There was no inhibition of Jm_{amm} except for a slight reduction in the anterior intestine of fed fish (Figs. 4, 5), which greatly weakens the case for involvement of NKCC in the apical uptake step. Further evidence against NKCC involvement was a lack of stimulation of either Jm_{amm} or Js_{amm} by elevated mucosal [Na^+] (HMN) (Figs. 1, 2), and a lack of stimulation by low mucosal [K^+] (LMK) (Figs. 7, 8). Indeed, in some sections, inhibitions were observed, whereas if NKCC was involved, increased ammonia transport would be expected to result from both treatments. The inhibitory actions of LMSN could be interpreted as support for NKCC, but equally well could have resulted from a reduction of intracellular [Na^+], tending to

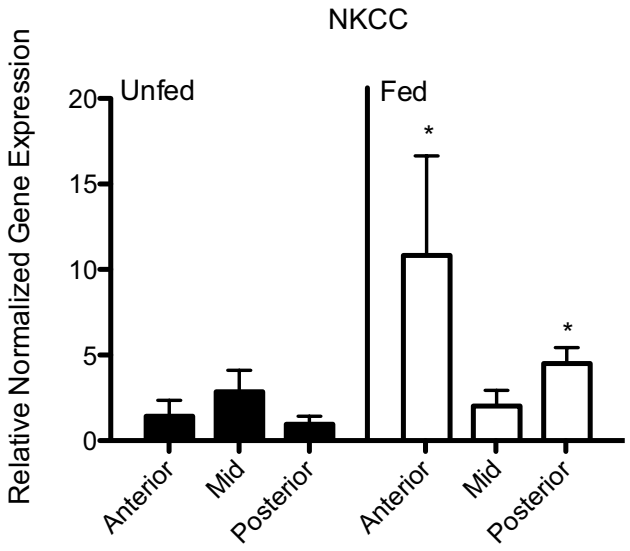

Fig. 10 Relative normalized gene expression for the NKCC rainbow trout isoform for unfed and fed fish. "Asterisk" significant ($P < 0.05$) comparing fed sections to the respective unfed sections ($N = 5$ each section)

slow down NKA, which provides the overall driving force for ammonia transport, as discussed subsequently.

One caveat with respect to the lack of an inhibitory effect of bumetanide on Jm_{amm} is that this result may have been confounded by the required presence of the 0.1% DMSO vehicle. DMSO by itself generally inhibited both Jm_{amm} and Js_{amm}, without effects on Jt_{amm} (Table 1). As Jm_{amm} values were generally close to zero in the presence of DMSO, a true inhibitory effect of bumetanide + 0.1% DMSO (relative to 0.1% DMSO alone) on Jm_{amm} would have manifested as a switch to negative values, but this was generally not seen (Figs. 4, 5). However, since bumetanide strongly suppressed Jt_{amm}, this might have limited the gradient for unidirectional ammonia backflux from tissue to lumen, preventing the response. The reason why 0.1% DMSO inhibited Jm_{amm} and Js_{amm} is unclear, as this vehicle usually increases membrane permeability (Notman et al. 2006). Perhaps, there are normally significant backfluxes of ammonia at both surfaces, such that the observed Jm_{amm} and Js_{amm} (which are net fluxes) are reduced. Similarly, the reason why bumetanide inhibited endogenous ammonia production (Jt_{amm}) is unclear. Intestinal N-metabolism is complex (reviewed by Bergen and Wu 2009; Taylor et al. 2011). One possibility

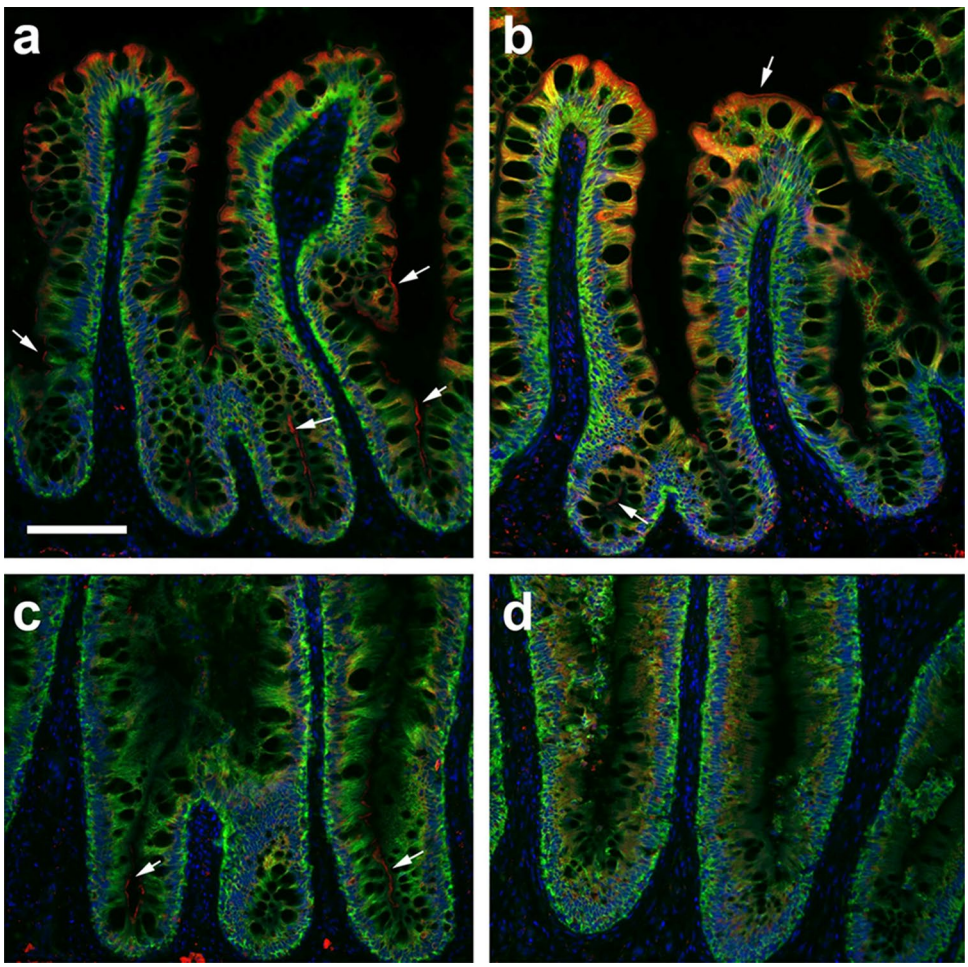

Fig. 11 Double immunofluorescence localization of NKCC/NCC (red) and NKA (α subunit, green) with DAPI nuclear staining of the anterior (**a**, **b**) and posterior (**c**, **d**) intestine of fed (**a**, **c**) and unfed (**b**, **d**) rainbow trout. Arrows indicate brush border staining. Scale bar = 100 µm

is reduced glutamine transport into mitochondria. At the concentration used here, bumetanide has been reported to act as a competitive inhibitor of glutamate transport into synaptic vesicles (Roseth et al. 1995). Glutamate dehydrogenase and glutaminase are thought to be the major routes of endogenous ammonia production in trout intestine (Rubino et al. 2014), so reduction of mitochondrial glutamate supply by bumetanide may have led to the reduction of Jt_{amm} and, therefore, Js_{amm}.

Overall, the present data provide little support for ammonia uptake across the mucosal surface of the trout intestine by NKCC, except perhaps in the anterior intestine after feeding where NKCC is markedly upregulated. In comparable mammalian models such as a colonic crypt cell line, the role of apical NKCC appears to be solely secretory so as to promote ammonia backflux into the lumen, thereby preventing ammonia levels in the portal bloodstream from rising too high (Worrell et al. 2008). Similarly, in the rumen of sheep, there appears to be no role for NKCC in ammonia absorption, and the interaction of K^+ with ammonia uptake can be explained by NH_4^+ entry through apical K^+ channels (reviewed by Abdoun et al. 2007).

Are K^+ channels involved in ammonia transport?

The findings of Abdoun et al. (2007) on ammonia transport across the rumen prompted our interest in the potential involvement of K^+ channels, and led to the experiments with barium, a broad-spectrum inhibitor of K^+ channels (Yellen 1987; Taglialatela et al. 1993; Choe et al. 2000). HMB has been reported to strongly inhibit both ammonia and K^+ absorption in the perfused rat intestine in vivo (Hall et al. 1992). Mucosal quinidine (another broad-spectrum K^+ channel blocker) reduced ammonia absorption across the sheep rumen in vitro (Bödeker and Kemkowski 1996). In most trout preparations, both HMB and HSB strongly inhibited Jm_{amm} and Js_{amm} (Figs. 7, 8) without effects on Jt_{amm} (Fig. 9). The anterior intestine was again an exception (Figs. 7a, d, 8a).

K^+ channels are often highly permeable to NH_4^+ (Yellen 1987; Choe et al. 2000). Ion flow through K^+ channels is determined by the prevailing electrochemical gradients (MacKinnon 2003). Considering the high intracellular $[K^+]$ and low mucosal $[K^+]$, the electrochemical gradient would likely be in the secretory direction for K^+ through apical channels in the intestine (Loretz 1995; Movileanu et al. 1998). Indeed, in a marine teleost, an apical barium-sensitive K^+ channel-mediating K^+ secretion into the lumen has been identified (Musch et al. 1982; Loretz 1995). However, measured tissue ammonia concentrations are approximately twofold higher than the mucosal fluid concentrations in trout gut sac preparations (Rubino et al. 2014), and the potential difference across the apical membrane of enterocytes should be highly negative inside (see Bödeker and Kemkowski 1996; Abdoun et al. 2007). Therefore, there should be a strong electrochemical gradient for NH_4^+ uptake through K^+ channels in the apical membrane, which would explain why HMB blocks Jm_{amm} and Js_{amm}. The presence of basolateral K^+ channels also seems likely, though there is also evidence for basolateral K^+ exit by K^+:Cl^- co-transport in the intestine of marine teleosts (Smith et al. 1980; Loretz 1995; Movileanu et al. 1998; Grosell 2011). HSB would block basolateral K^+ channels, but it seems unlikely that the prevailing electrochemical gradient would favor NH_4^+ efflux though such channels. More probably, blockade of these channels by HSB would increase intracellular $[K^+]$, thereby reducing NKA activity, and, therefore, the net driving force on NH_4^+ transport, explaining the inhibition of Jm_{amm} and Js_{amm}. Overall, the present results suggest that ammonia uptake across the mucosal surface of the trout intestine occurs in part via NH_4^+ entry through apical K^+ channels.

What is the role of NKA in ammonia transport?

Ouabain is a potent and irreversible inhibitor of NKA (Albers et al. 1968), so its actions in reducing both Jm_{amm} (Fig. 1) and Js_{amm} (Fig. 2) without effects on Jt_{amm} (Fig. 3) in most sections were in accord with the findings of Rubino et al. (2015), where only Js_{amm} was monitored. The inhibitory actions of LMSN (Figs. 1, 2) can also be explained by a slowing of NKA. These results strongly suggest that NKA plays an important role in energizing ammonia absorption. This finding also agrees with mammalian studies where anaerobiosis, 2,4-dinitrophenol, and sodium cyanide inhibited ammonia absorption in the ileum (Mossberg and Ross 1967), while ouabain inhibited ammonia secretion in colonic crypt cells (Worrell et al. 2008). It is interesting that the inhibitory effects of ouabain were reduced by feeding, which is known to cause an upregulation of intestinal NKA activity in fish (Kamunde and Wood 2003; Turner and Bucking 2017). The primary role of NKA is likely to establish the overall electrochemical gradient for transport. To the extent that apical NH_4^+ uptake by NKCC is involved, the low intracellular $[Na^+]$ and negative intracellular potential will energize this process. Similarly, the negative potential will help to drive NH_4^+ entry through apical K^+ channels. While we suggest that transport across the membrane is facilitated by NKA, paracellular transport of ammonia due to movement of water across the epithelium due to osmotic gradients (Grosell 2011) and transcellular transport of water through aquaporins (e.g., AQP1, Wood and Grosell 2012) cannot be discounted. Furthermore, Rubino et al. (2015) identified reduced fluid transport rates across the intestine in gut sacs when using ouabain. Therefore, this reduction in

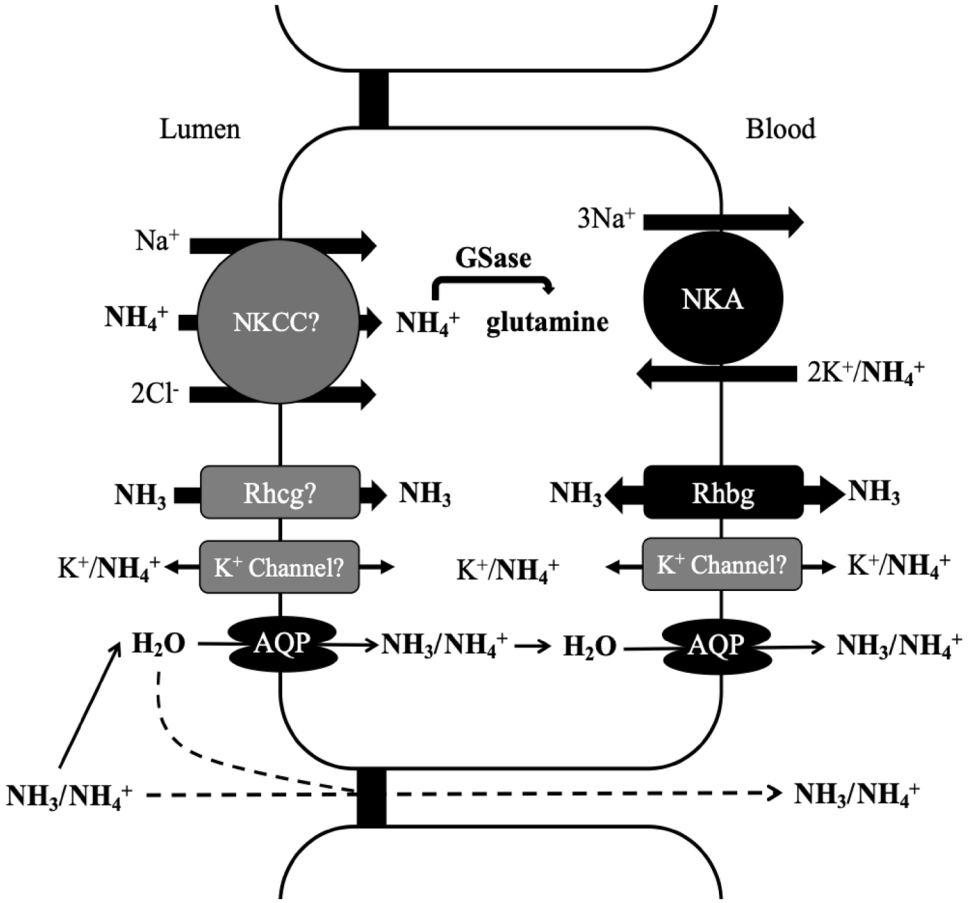

Fig. 12 Updated schematic diagram as a conceptual model for transcellular and paracellular ammonia transport for all sections of the intestine, revised from earlier version of Rubino et al. (2015). Routes for ammonia uptake are energized by basolateral NKA providing the electrochemical gradients for secondary active transport. Ammonia is believed to occupy K^+ transport sites on various transporters at both the apical and basolateral surface, though with less involvement of NKCC than previously suggested. It is possible for ammonia to also enter intestinal cells through either an apical or basolateral Rh glycoprotein. Alternative routes of uptake through solvent drag via fluid transport occurring through osmosis, or water uptake through aquaporins (Wood and Grosell 2012) may also occur. Once inside the cells, ammonia detoxification enzymes, such as GSase, may reduce intracellular ammonia concentrations (Bucking and Wood 2012; Rubino et al. 2014)

fluid transport may contribute to the reduction in ammonia flux observed when this inhibitor is applied.

At the same time, basolateral NKA may play a very different role at the blood side, that of NH_4^+ uptake ('scavenging') from the portal blood so as to prevent circulating levels of ammonia from rising too high after feeding, and to ensure that there is a ready supply of substrate for glutamine synthesis in the enterocytes (Bergen and Wu 2009; Taylor et al. 2011; Wilson et al. 2013). This would occur by NH_4^+ competition at the extracellular K^+ binding site on the enzyme. In support of this idea, we found that NH_4^+ was just as effective as K^+ in supporting intestinal NKA activity, a phenomenon that was not seen with gill NKA (Table 2). The inability of NH_4^+ to support gill NKA activity confirms previous observations on trout (Salama et al. 1999; Wood and Nawata 2011), though in several other teleost species, gill NKA activity can be strongly increased by NH_4^+ (Randall et al. 1999; Wood et al. 2013, 2014). We are aware of no previous studies on NH_4^+ effects on intestinal NKA in fish. By this model, high NH_4^+ levels in the intestinal blood after feeding might help to improve the electrochemical gradient for NH_4^+ absorption, which may direct more ammonia into amino acid synthesis by the intestinal tissue through scavenging from the portal blood. This starts with the trapping of ammonia into glutamine by glutamine synthetase, which increases in activity in response to feeding in the intestine (Bucking and Wood 2012; Bucking et al. 2013b). Glutamine can then shuttle amino groups to other amino acids and can provide energy to the intestinal cells for oxidation or gluconeogenesis.

Concluding remarks and future directions

Rubino et al. (2015) presented a preliminary, rather speculative model describing ammonia transport in the intestinal tract of rainbow trout (see their Fig. 8). The present study clarifies and expands that model (Fig. 12). While the proposal of an apical NKCC is confirmed, the present more detailed analysis suggests that this transporter is not as important in ammonia absorption as earlier hypothesized, except perhaps in the anterior intestine. Rather, the interaction with K^+ seems to occur because $NH_4^+$is taken up through barium-sensitive K^+ channels on the apical surface. Mucosal NH_4^+ uptake via both NKCC and K^+ channels is energized by basolateral NKA, which plays an additional role in scavenging NH_4^+ on the serosal surface. This occurs by transport on the extracellular K^+ binding site of NKA,

thereby ensuring intracellular substrate for amino acid synthesis in the intestinal tissue. $NH_4^+$is equally effective as K^+ in supporting the activity of the enzyme; this may become important when ammonia levels in the intestinal circulation are elevated after feeding.

However, many uncertainties remain, some of which can best be solved by electrophysiological studies using Ussing chambers and patch clamping, approaches which have proven very useful in understanding how Na^+, Cl^-, and HCO_3^- are transported in the gastrointestinal tracts of marine teleosts (Loretz 1995; Grosell 2011). However, some important questions can be profitably attacked using the simple gut sac approach. Principal among these is the potential role of non-ionic diffusion of NH_3 along PNH_3 gradients, perhaps facilitated by Rh proteins. The role of non-ionic diffusion issue has been extensively investigated in the gills of fish, yet remains controversial (Wilkie 2002; Wright and Wood 2009; Ip and Chew 2010).This mechanism has not yet been examined in the fish intestine, despite substantial evidence that it plays a role in ammonia transport in the mammalian gastrointestinal tract (Swales et al. 1970; Castell and Moore 1971; Brown et al. 1975; Abdoun et al. 2007). Non-ionic diffusion can be examined by establishing fixed PNH_3 gradients across gut sac preparations, far more easily than across the gills. Furthermore, Rubino et al. (2015) argued that ammonia movement by solvent drag may also be important in the fish intestine; again, this can be addressed quite easily by establishing fixed osmotic gradients across gut sac preparations (e.g., Wood and Grosell 2012). Our understanding of ammonia transport and metabolism in the fish intestine remains in its infancy. This is a rich area for future investigation.

Acknowledgements Special thanks to Drs. Grant McClelland and Graham Scott at McMaster University for allowing the use of their lab space to complete some of the final experiments. Three anonymous reviewers provided constructive comments that improved the MS. This work was supported by NSERC Discovery grants (NSERC RGPIN 473-2012 and RGPIN 03843-2017) to CMW who was also supported by the Canada Research Chair Program (Award 203776). JMW was supported by NSERC DG RGPIN 04289-2014.

References

Abdoun K, Stumpff F, Martens H (2007) Ammonia and urea transport across the rumen epithelium: a review. Anim Health Res Rev 1–2:43–59

Albers RW, Koval GJ, Siegel GJ (1968) Studies on the interaction of ouabain and other cardio-active steroids with sodium-potassium activated adenosine triphosphatase. Mol Pharmacol 4:324–336

Bergen WG, Wu G (2009) Intestinal nitrogen recycling and utilization in health and disease. J Nutr 139:821–825

Bödeker D, Kemkowski J (1996) Participation of NH_4^+ in total ammonia absorption across the rumen epithelium of sheep (*Ovis aries*). Comp Biochem Physiol A 114:305–310

Brett JR, Zala CA (1975) Daily pattern of nitrogen excretion and oxygen consumption of sockeye salmon (*Oncorhynchus nerka*) under controlled conditions. J Fish Res Board Can 32:2479–2486

Brown RL, Gibson JA, Fenton JCB, Snedden W, Clark ML, Sladen GE (1975) Ammonia and urea transport by the excluded human colon. Clin Sci Mol Med 48:279–287

Bucking C, Wood CM (2008) The alkaline tide and ammonia excretion after voluntary feeding in freshwater rainbow trout. J Exp Biol 211:2533–2541

Bucking C, Wood CM (2012) Digestion of a single meal affects gene expression and enzyme activity in the gastrointestinal tract of freshwater rainbow trout. J Comp Physiol B 182:341–350

Bucking C, Edwards SL, Tickle P, Smith CP, McDonald MD, Walsh PJ (2013a) Immunohistochemical localization of urea and ammonia transporters in two confamilial fish species, the ureotelic gulf toadfish (*Opsanus beta*) and the ammoniotelic plainfin midshipman (*Porichthys notatus*). Cell Tissue Res 352:623–637

Bucking C, Lemoine CM, Craig PM, Walsh PJ (2013b) Nitrogen metabolism of the intestine during digestion in a teleost fish, the plainfin midshipman (*Porichthys notatus*). J Exp Biol 216:2821–2832

Castell DO, Moore EW (1971) Ammonia absorption from the human colon: the role of nonionic diffusion. Gastroenterology 60:33–42

Choe H, Sackin H, Palmer LG (2000) Permeation properties of inward-rectifier potassium channels and their molecular determinants. J Gen Physiol 115:391–404

Grosell M (2011) The role of the gastrointestinal tract in salt and water balance. In: Grosell M, Farrell AP, Brauner CJ (eds) The multifunctional gut, fish physiology, vol 30. Academic Press, San Diego, pp 135–164

Grosell M, Jensen FB (1999) NO_2^- uptake and HCO_3^- excretion in the intestine of the European flounder (*Platichthys flesus*). J Exp Biol 202:2103–2110

Hall MC, Koch MO, McDougal WS (1992) Mechanism of ammonium transport by intestinal segments following urinary diversion: evidence for ionized NH_4^+ transport via K^+-pathways. J Urol 148:453–457

Handlogten ME, Hong SP, Zhang L, Vander AW, Steinbaum ML, Campbell-Thompson M, Weiner ID (2005) Expression of the ammonia transporter proteins Rh B glycoprotein and Rh C glycoprotein in the intestinal tract. Am J Physiol Gastrointest Liver Physiol 288:G1036–G1047

Hiroi J, McCormick SD, Ohtani-Kaneko R, Kaneko T (2005) Functional classification of mitochondrion-rich cells in euryhaline Mozambique tilapia (*Oreochromis mossambicus*) embryos, by means of triple immunofluorescence staining for Na+/K+-ATPase, Na+/K+/2Cl-cotransporter and CFTR anion channel. J Exp Biol 208:2023–2036

Hosoi R, Matsuda T, Asano S, Nakamura H, Hashimoto H, Takuma K, Baba A (2002) Isoform-specific up-regulation by ouabain of Na+, K+-ATPase in cultured rat astrocytes. J Neurochem 69:2189–2196

Ip YK, Chew SF (2010) Ammonia production, excretion, toxicity, and defense in fish: a review. Front Physiol 1:134

Kamunde C, Wood CM (2003) The influence of ration size on copper homeostasis during sublethal dietary copper exposure in juvenile rainbow trout, *Oncorhynchus mykiss*. Aquat Toxicol 62:235–254

Karlsson A, Eliason EJ, Mydland LT, Farrell AP, Kiessling A (2006) Postprandial changes in plasma free amino acid levels obtained simultaneously from the hepatic portal vein and the dorsal aorta in rainbow trout (*Oncorhynchus mykiss*). J Exp Biol 209:4885–4894

Kinne R, Kinne-Saffran E, Schütz H, Schölermann B (1986) Ammonium transport in medullary thick ascending limb of rabbit kidney: involvement of the Na^+, K^+, $Cl(^-)$-co-transporter. J Membr Biol 94:279–284

Loretz CA (1995) Electrophysiology of ion transport in teleost intestinal cells. In: Wood CM, Shuttleworth TJ (eds) Cellular and molecular approaches to fish ionic regulation, fish physiology, vol 14. Academic Press, San Diego, pp 25–56

MacKinnon R (2003) Potassium channels. FEBS Lett 555:62–65

Marshall WS (1986) Independent Na^+ and Cl^- active transport by urinary bladder epithelium of brook trout. Am J Physiol 250:227–234

McCormick SD (1993) Methods for non-lethal gill biopsy and measurement of Na+, K+-ATPase activity. Can J Fish Aquat Sci 50:656–658

Mossberg SM, Ross G (1967) Ammonia movement in the small intestine: preferential transport by the ileum. J Clin Investig 46:490–498

Movileanu L, Flonta ML, Mihailescu D, Frangopol PT (1998) Characteristics of ionic transport processes in fish intestinal epithelial cells. Biosystems 45:123–140

Musch MW, Orellana SA, Kimberg LS, Field M, Halm DR, Krasny EJ Jr, Frizzell RA (1982) Na^+, K^+, $2Cl^-$ co-transport in the intestine of a marine teleost. Nature 300:351–353

Nadella SR, Patel D, Ng A, Wood CM (2014) An in vitro investigation of gastrointestinal Na^+ uptake mechanisms in freshwater rainbow trout. J Comp Physiol B 184:1003–1019

Nawata CM, Hung CYC, Tsui TKN, Wilson JM, Wright PA, Wood CM (2007) Ammonia excretion in rainbow trout (*Oncorhynchus mykiss*): evidence for Rh glycoprotein and H^+-ATPase involvement. Physiol Genom 31:463–474

Notman R, Noro M, O'Malley B, Anwar J (2006) Molecular basis for dimethylsulfoxide (DMSO) action on lipid membranes. J Am Chem Soc 128:13982–13983

Pelster B, Wood CM, Speers-Roesch B, Driedzic WR, Almeida-Val V, Val AL (2015) Gut transport characteristics in herbivorous and carnivorous serrasalmid fish from ion poor Rio Negro water. J Comp Physiol B 185:225–241

Randall DJ, Wilson JM, Peng KW, Kok TWK, Kuah SSL, Chew SF, Ip YK (1999) The mudskipper, *Periophthalmodon schlosseri*, actively transports NH_4^+ against a concentration gradient. Am J Physiol 277:R1562–R1567

Rubino JG, Zimmer AM, Wood CM (2014) An in vitro analysis of intestinal ammonia handling in fasted and fed freshwater rainbow trout (*Oncorhynchus mykiss*). J Comp Physiol B 184:91–105

Rubino JG, Zimmer AM, Wood CM (2015) Intestinal ammonia transport in freshwater and seawater acclimated rainbow trout (*Oncorhynchus mykiss*): evidence for a Na^+ coupled uptake mechanism. Comp Biochem Physiol A 183:45–56

Salama A, Morgan IJ, Wood CM (1999) The linkage between Na^+ uptake and ammonia excretion in rainbow trout: kinetic analysis, the effects of $(NH_4)_2SO_4$ and NH_4HCO_3 infusion and the influence of gill boundary layer pH. J Exp Biol 202:697–709

Smith CP, Smith PL, Welsh MJ, Frizzell RA, Orellana SA, Field M (1980) Potassium transport by the intestine of the winter flounder *Pseudopleuronectes americanus*: evidence for KCl co-transport. Bull Mt Desert Island Biol Lab 20:92–96

Swales JD, Tange JD, Wrong OM (1970) The influence of pH, bicarbonate and hypertonicity on the absorption of ammonia from the rat intestine. Clin Sci 39:769–779

Taglialatela M, Drewe JA, Brown AM (1993) Barium blockade of a clonal potassium channel and its regulation by a critical pore residue. Mol Pharmacol 44:180–190

Taylor JR, Cooper CA, Mommsen TP (2011) Implications of GI function for gas exchange, acid–base balance and nitrogen metabolism. In: Grosell M, Farrell AP, Brauner CJ (eds) The multifunctional gut, fish physiology, vol 30. Academic Press, San Diego, pp 213–259

Thrane VR, Thrane AS, Wang F, Cotrina ML, Smith NA, Chen M, Xu Q, Kang N, Fujita T, Nagelhus EA, Nedergaard M (2013) Ammonia triggers neuronal disinhibition and seizures by impairing astrocyte potassium buffering. Nat Med 19:1643–1648

Turner LA, Bucking C (2017) The interactive effect of digesting a meal and thermal acclimation on maximal enzyme activities in the gill, kidney, and intestine of goldfish (*Carassius auratus*). J Comp Physiol B 187:959–972

Weiner ID (2006) Expression of the non-erythroid Rh glycoproteins in mammalian tissues. Transfus Clin Biol 13:159–163

Westlund A, Haggstrom L (1998) Ammonium ion transport by the Na^+K^+2Cl-cotransporter induces apoptosis in hybridoma cells. Biotechnol Lett 20(1):87–90

Wilkie MP (2002) Ammonia excretion and urea handling by fish gills: present understanding and future research challenges. J Exp Zool 293:284–301

Wilson JM, Leitão A, Gonçalves AF, Ferreira C, Reis-Santos P, Fonseca AV, da Silva JM, Antunes JC, Pereira-Wilson C, Coimbra J (2007) Modulation of branchial ion transport protein expression by salinity in glass eels (*Anguilla anguilla* L.). Mar Biol 151(5):1633–1645

Wilson JM, Moreira-Silva J, Delgado IL, Ebanks SC, Vijayan MM, Coimbra J, Grosell M (2013) Mechanisms of transepithelial ammonia excretion and luminal alkalinization in the gut of an intestinal air-breathing fish, *Misgurnus anguilliacaudatus*. J Exp Biol 216(4):623–632

Wolf K (1963) Physiological salines for fresh-water teleosts. Progress Fish Cult 25:135–140

Wood CM, Grosell M (2012) Independence of net water fluxes from paracellular permeability in the intestine of *Fundulus heteroclitus*, a euryhaline teleost. J Exp Biol 215:508–517

Wood CM, Nawata CM (2011) A nose-to-nose comparison of the physiological and molecular responses of rainbow trout to high environmental ammonia in sea water versus fresh water. J Exp Biol 214:3557–3569

Wood CM, Nawata CM, Wilson JM, Laurent P, Chevalier C, Bergman HL, Bianchini A, Maina JN, Johannsson OE, Bianchini LF, Kavembe GD, Papah MB, Ojoo RO (2013) Rh proteins and NH_4^+-activated Na^+ATPase in the Magadi Tilapia (*Alcolapia grahami*), a 100% ureotelic teleost fish. J Exp Biol 216:2998–3007

Wood CM, Robertson LM, Johannsson OE, Val AL (2014) Mechanisms of Na^+ uptake, ammonia excretion, and their potential linkage in native Rio Negro tetras (*Paracheirodon axelrodi*, *Hemigrammus rhodostomus*, and *Moenkhausia diktyota*). J Comp Physiol B 184:877–890

Wood CM, Liew HJ, De Boeck G, Hoogenboom JL, Anderson WG (2019) Nitrogen handling in the elasmobranch gut: a role for microbial urease. J Exp Biol 222:194787 **(in press)**

Worrell RT, Merk L, Matthews JB (2008) Ammonium transport in the colonic crypt cell line, T84: role for rhesus glycoproteins and NKCC1. Am J Physiol Gastrointest Liver Physiol 294:G429–G440

Wright PA, Wood CM (2009) A new paradigm for ammonia excretion in aquatic animals: role of Rhesus (Rh) glycoproteins. J Exp Biol 212:2303–2312

Xu JC, Lytle C, Zhu TT, Payne JA, Benz E Jr, Forbush B 3rd (1994) Molecular cloning and functional expression of the bumetanide-sensitive Na–K–Cl cotransporter. Proc Natl Acad Sci 91:2201–2205

Yellen G (1987) Permeation in potassium channels: implications for channel structure. Ann Rev Biophys Biophys Chem 16:227–246

Zimmer A, Nawata CM, Wood CM (2010) Physiological and molecular analysis of the interactive effects of feeding and high environmental ammonia on branchial ammonia excretion and Na^+ uptake in freshwater rainbow trout. J Comp Physiol B 180:1191–1204